GOING TO THE EXTREMES

AN INTERCOMPARISON OF MODEL-SIMULATED HISTORICAL AND FUTURE CHANGES IN EXTREME EVENTS

CLAUDIA TEBALDI[1] KATHARINE HAYHOE[2,3] JULIE M. ARBLASTER[4,5] and GERALD A. MEEHL[4]

[1]*Institute for the Study of Society and Environment, National Center for Atmospheric Research (NCAR), PO BOX 3000, Boulder, CO 80301*
E-mail: tebaldi@ucar.edu
[2]*Department of Atmospheric Sciences,University of Illinois at Urbana-Champaign, Urbana,IL*
[3]*Department of Geosciences, Texas Tech University,Lubbock, TX*
[4]*Climate and Global Dynamics Division, NCAR,Boulder, CO*
[5]*Bureau of Meteorology Research Centre, Melbourne, Australia*

Abstract. Projections of changes in climate extremes are critical to assessing the potential impacts of climate change on human and natural systems. Modeling advances now provide the opportunity of utilizing global general circulation models (GCMs) for projections of extreme temperature and precipitation indicators. We analyze historical and future simulations of ten such indicators as derived from an ensemble of 9 GCMs contributing to the Fourth Assessment Report of the Intergovernmental Panel on Climate Change (IPCC-AR4), under a range of emissions scenarios. Our focus is on the consensus from the GCM ensemble, in terms of direction and significance of the changes, at the global average and geographical scale. The climate extremes described by the ten indices range from heat-wave frequency to frost-day occurrence, from dry-spell length to heavy rainfall amounts. Historical trends generally agree with previous observational studies, providing a basic sense of reliability for the GCM simulations. Individual model projections for the 21st century across the three scenarios examined are in agreement in showing greater temperature extremes consistent with a warmer climate. For any specific temperature index, minor differences appear in the spatial distribution of the changes across models and across scenarios, while substantial differences appear in the relative magnitude of the trends under different emissions rates. Depictions of a wetter world and greater precipitation intensity emerge unequivocally in the global averages of most of the precipitation indices. However, consensus and significance are less strong when regional patterns are considered. This analysis provides a first overview of projected changes in climate extremes from the IPCC-AR4 model ensemble, and has significant implications with regard to climate projections for impact assessments.

1. Introduction

In recent years, the need for regional-scale projections of climate variables and thresholds that are directly relevant to impacts researchers and stake-holders has been strongly voiced (Hare, 2006). Since the IPCC Third Assessment Report (Houghton et al., 2001), climate change detection and projections of future change are no longer relegated to global averages and have expanded to include extremes (Hegerl et al., 2004). Substantial progress in both global and regional modeling

Climatic Change (2006)
DOI: 10.1007/s10584-006-9051-4

at medium to high resolution (Duffy et al., 2003; Govindasamy et al., 2003)[1] has provided the basis for an increasing number of studies that attempt to characterize expected changes at local scales. Recent modeling efforts have also provided us with the ability to characterize changes in terms of indices with greater relevance to impacts than the traditional climate model outputs of mean temperature, precipitation and sea level pressure (e.g., Hayhoe et al., 2004; Meehl and Tebaldi, 2004; Meehl et al., 2004; Meehl et al., 2005a).

A primary concern in estimating impacts from climate change are the potential changes in variability and hence extreme events that could accompany global climate change. Extreme events such as heatwaves, heavy rain or snow events and droughts are responsible for a disproportionately large part of climate-related damages (Kunkel et al., 1999; Easterling et al., 2000; Meehl et al., 2000) and hence are of great concern to the impact community and stakeholders (Katz et al., 2005; Negri et al., 2005). Katz and Brown (1994) first suggested that the sensitivity of extremes to changes in mean climate may be greater than one would assume from simply shifting the location of the climatological distributions. Since then, observations of historical changes as well as future projections confirm that changes in the distributional tails of climate variables may not occur in proportion to changes in the mean, particularly for precipitation, and may not be symmetric in nature, as demonstrated by differential changes in maximum vs. minimum temperatures (e.g., Kharin and Zwiers, 2005; Robeson, 2004; Tank and Konnen, 2003; Easterling et al., 2000).

Over the past decade, a number of studies have attempted to identify observed and projected future changes in extreme events. These have employed a range of temperature and precipitation data that included return periods (e.g., Ekstrom et al., 2005; Semmler and Jacob, 2004; Wehner, 2004); frequency-duration-intensity indices (Adamowski and Bougadis, 2003; Khaliq et al., 2005); multivariate statistics (Bohm et al., 2004; Huth and Pokorna, 2005); and indices based on frequency and variance (Palmer and Raisanen, 2002; Meehl and Tebaldi, 2004).

The landmark effort by Frich et al. (2002, henceforth F02) was instrumental in setting the stage for a coordinated effort to identify and monitor indices of extreme events, both as observed and simulated. In F02, ten indicators of extreme events were chosen based on their ability to summarize a wide spectrum of climate extreme characteristics, and their robustness in the face of both measurement and predictive uncertainty.[2] Robustness is to be viewed as the result of a trade-off between the extreme and therefore infrequent nature of the phenomena described and the availability in the climate records of enough instances of these phenomena to allow a stable estimate of their frequency and intensity. The resulting ten indicators may be seen as "not as extreme" as they could be, given the necessary criteria of sufficient occurrences over the historical observational period, but it is exactly this quality that leaves open the possibility of using climate model output for their computation. Inevitably, because of their finite and still relatively coarse

resolution, climate models are not expected to represent extreme weather events with the intensity and frequency comparable to what is observed, particularly for precipitation-related events (Kiktev et al., 2003; Raisanen and Joelsoon, 2002). Nonetheless, the "less extreme" nature of these indices, together with definitions involving climatologies that are model-specific, justifies application of AOGCM output to investigate changes in their behavior, and taking the simulated future changes as indicative of what we can expect from future climate extremes.

The goal of this study is to survey the most recent projections of climate extremes provided by the latest state-of-the-art AOGCMs, as contributed to a common archive hosted by PCMDI[3] as part of the activities sponsored by the IPCC leading up to its Fourth Assessment Report. Besides standard fields that are the direct output of the model simulations, modeling centers have agreed to compute the ten indicators defined by F02 for the 20th century climate (historical) experiments and as projected for a range of future SRES emission scenarios. Thus, our objective here is to analyze these quantities as provided by the modeling centers. There is some indication that the methodology used to calculate at least one of the F02 temperature indices, warm nights, results in a bias in the calculation of 20th century trends (Zhang et al., 2005). However, as the purpose of this study is to examine the trends in the indices as defined by the IPCC for calculation by the AR4 modeling community, we remain with the original definition although noting this discrepancy for the purposes of the interpretation of these results.

This multi-model dataset and consistent representation of the ten extreme indices enables us to compare the historical simulation results to the observed trends reported in F02 and to analyze projected changes within and across models. It is important to note that a new study has been recently performed and will soon become available (Alexander et al., 2005), updating the F02 analysis into a spatially comprehensive and current set of estimates of the observed trends in the ten indicators. A more quantitative evaluation of the models' fidelity in simulating trends in the 20th century extremes awaits release of that dataset. Here, we cite qualitative comparisons with previously published estimates of changes in relevant extremes that provide context for the model projections of future changes of extremes (Table II).

The paper is organized as follows. In Section 2 we briefly describe the ten indicators and their significance. In Section 3 we focus on temperature extremes. We first compare model-simulated historical runs to the observational changes presented in F02 in terms of time series of global and hemispheric averages. We then proceed to characterize our confidence in the sign of the future expected changes, by comparing the different model results and analysing commonalities and differences in the future projections under the range of available SRES scenarios. We then focus on geographical patterns, discussing the model consensus in terms of sign and significance of the projected changes for the end of the 21st century. Section 4 mirrors Section 3, but analyzes the five indicators of precipitation extremes

TABLE I
The nine Atmosphere-Ocean General Circulation Models featured in our analysis

Modeling center	AOGCM	Climate sensitivity (TCR)
National Center for Atmospheric Research (USA)	CCSM3	1.46
Météo-France & Centre National de Recherches Météorologiques (France)	CNRM-CM3	1.57
US Dept. of Commerce & National Oceanic and Atmospheric Administration & Geophysical Fluid Dynamics Laboratory (USA)	GFDL-CM2.0	1.60
US Dept. of Commerce & National Oceanic and Atmospheric Administration & Geophysical Fluid Dynamics Laboratory (USA)	GFDL-CM2.1	1.50
Institute for Numerical Mathematics (Russia)	INM-CM3	1.57
Center for Climate System Research & National Institute for Environmental Studies & Frontier Research Center for Global Change (JAPAN)	MIROC3.2(medres)	2.11
Center for Climate System Research & National Institute for Environmental Studies & Frontier Research Center for Global Change (JAPAN)	MIROC3.2(hires)	NA
Department of Energy & National Center for Atmospheric Research (USA)	PCM	1.32
Meteorological Research Institute & Japan Meteorological Agency (Japan)	MRI-CGCM2	0.97

instead. Section 5 gives a brief overview of the geographical changes simulated by the models over the 20th century, for comparison with the future changes. Section 6 summarizes the results.

At the time of writing nine models have provided the ten extremes indicators to the PCMDI archive (see Table I). Although only a subset of all models that have contributed to the archive, the preliminary results here described will nonetheless provide a reasonably representative assessment of what might be expected from the full ensemble of model simulations. The models with extremes indices currently available are the DOE/NCAR Parallel Climate Model (PCM; Washington et al., 2000) and Coupled Climate System Model (CCSM3)[4], the CCSR MIROC medium and high resolution models (Hasumi and Emori, 2004)[5], INM-CM3 (Diansky et al., 2002), CNRM-CM3,[6] GFDL-CM2.0, GFDL-CM2.1 (Delworth et al., 2002; Dixon et al., 2003) and MRI-CGCM2 (Yukimoto et al., 2001). Model grid resolutions vary from relatively coarser (INMCM3, $5^\circ \times 4^\circ$) to relatively finer (MIROC hires, $\sim 1.125^\circ$). Model simulations are available for the historical period, as well as for three future SRES emissions scenarios: A2 (higher), A1B (mid-range) and B1 (lower) (Nakicenovic et al., 2000). Projected end-of-21st century carbon emissions for these scenarios, driven by variations in underlying assumptions regarding pop-

ulation, technology and energy use, range from 5 GtC/yr for B1 up to 29 GtC/yr for A2. Corresponding atmospheric CO_2 concentrations in 2100 lie between ∼500 to ∼900 ppm.

Of the nine AOGCMs with F02 extremes indices available, there are multiple ensemble members of the climate of the 20th century experiment (20C3M) for five of the models; four from the PCM, three each from MIROC3.2 (medres), GFDL-CM2.0 and GFDL-CM2.1 and five from MRI-CGCM2.3.2. For the three 21st century experiments, multiple member ensembles are utilised from the PCM and MIROC3.2 (medres), with single runs from the remaining models. We aggregate all ensemble members from an individual model into an ensemble average, thus analysing a total of nine sets of simulations for each experiment (20C3M, SRESA2, SRESA1B and SRESB1). It should be noted that extremes indices were unavailable for the SRESA2 experiments of CCSM3 and MIROC3.2 (hires) models and the SRESB1 scenario of the MRI-CGCM2.3.2 model. Potential impacts on the results due to these omissions are discussed in later sections.

2. Ten Indicators of Climate Extremes

The indices chosen by F02 are intended to be representative of a wide variety of climate aspects for both subtropical and extratropical regions. Recent studies (Zhang et al., 2005; Alexander et al., 2005) have pointed out limitations of these definitions due to the choice of fixed thresholds, the use of a limited climatology (arguing that the indices have problematic statistical properties, or are not as robust as initially argued), or more generally, that they are not as relevant as claimed. However, our intent in this study is to document the indices as they were computed and submitted by the various modeling centers to the IPCC-AR4 data archive. Recomputing the indices is both not possible from the data available at the time of writing and beyond the scope of this study. Instead, we assess simulated historical and future projected trends using the original index definitions and compare these with historical observed trends as calculated by F02 using the same definitions.

Five indices describe temperature-related extremes:

1. Total number of frost days, defined as the annual total number of days with absolute minimum temperature below 0° C (*frost days*, or Fd in F02).
2. Intra-annual extreme temperature range, defined as the difference between the highest temperature of the year and the lowest (*xtemp range*, or ETR in F02).
3. Growing season length, defined as the length of the period between the first spell of five consecutive days with mean temperature above 5° C and the last such spell of the year (*growing season*, or GSL in F02).
4. Heat wave duration index, defined as the maximum period of at least 5 consecutive days with maximum temperature higher by at least 5° C than the

climatological norm for the same calendar day (*heat waves*, or HWDI in F02).

5. Warm nights, defined as the percentage of times in the year when minimum temperature is above the 90th percentile of the climatological distribution for that calendar day (*warm nights*, or Tn90 in F02).

While *frost days* and *growing season* have interesting interpretations only for extratropical (mid to high latitude) regions, describing mainly anomalies in the length of spring and fall seasons, the rest of the indices apply to all areas of the globe, sampling anomalies in daytime maxima or night-time minima and in the persistence of extremely hot days regardless of the lower variance encountered in tropical regions. Accordingly, in our analysis we calculated *frost days* and *growing season* only for regions poleward of $\pm 30^\circ$ latitude.

Five indices describe precipitation extremes:

1. Number of days with precipitation greater than 10 mm (*precip* $>$ 10, or R10 in F02).
2. Maximum number of consecutive dry days (*dry days*, or CDD in F02).
3. Maximum 5-day precipitation total (*5 day precip*, or R5d in F02).
4. Simple daily intensity index, defined as the annual total precipitation divided by the number of wet days (*precip intensity*, or SDII in F02).
5. Fraction of total precipitation due to events exceeding the 95th percentile of the climatological distribution for wet day amounts (*precip* $>$ 95th, or R95t in F02).

All indices except *dry days* measure changes in the intensity of rain. As for *dry days*, even if its definition is evocative of drought events, we regard it as an indicator of less extreme characteristics in the distribution of precipitation. Drought conditions are the effect of prolonged and complex sets of conditions, involving months- to years-long precipitation deficits and soil moisture characteristics that this simple index cannot represent. Rather, the index may be apt to measure the tendency – already hypothesized – towards longer dry spells separating intensified wet events, as suggested by the precipitation indices, and this particular association may be in fact more relevant to flood-related vulnerability studies due to heavy rainfall events such as have been observed over the continental U.S. (Kunkel, 2003).

It is clear from these definitions that we are not looking at extremely rare events, for which the computation of significant trends could be a priori hampered by the small sample sizes. In this respect, an important condition is that the thresholds for *heat waves*, *warm nights* and *precip* $>$95th be defined as percentiles of the climatologies computed from the same model's historical run between 1961 and 1990 (specifically based on 150 values, according to the definition in F02 that requires to use a 5-day window around the calendar date for the percentile computations).

With regard to the indices counting exceedances of percentile-based thresholds, and expanding on the caveat mentioned at the beginning of this section, we note the

following. It has been recently demonstrated (Zhang et al., 2005) that the use of a limited climatology introduces biases and discontinuities in the time series of these indices at the boundaries between in-base and out-of-base periods (which in our case are at 1961 and 1990). As already mentioned, recomputing the indices in order to correct these biases is beyond the scope of our study. On the other hand, given the qualitative aspect of our comparisons between observed and simulated trends, and the magnitude of the differences we detect between present and future rates of change, we believe these discontinuities are not critically affecting our results.

3. Temperature Extremes

3.1. GLOBAL AND HEMISPHERIC AVERAGES

Observationally-based extreme temperature indices analyzed by F02 were consistent with the idea of a general warming of the climate at the end of last century with greater warm extremes and less cold extremes. Significant trends for the observed globally averaged station records (mainly covering the northern hemisphere) were estimated for *frost days*, *xtemp range* (both decreasing during the last 5 decades of the 20th century), and *growing season* and *warm nights* (both increasing). The only globally averaged temperature index that lacked a significant trend was found to be *heat waves*.

F02's findings are consistent with other region-specific studies that used similar temperature indices for locations as diverse as the Caribbean (Peterson et al., 2002); China and South East Asia (Gong et al., 2004; Ryoo et al., 2004; Zhai et al., 2003; Gao et al., 2002); Oceania (Salinger and Griffiths, 2001); Europe (Prieto et al., 2004; Tank and Konnen, 2003); the Middle East (Nasrallah et al., 2003); and South America (Rusticucci and Barrucand, 2004). Most studies find increases in minimum temperatures and significant changes at the low (5–10%) and high (90–95%) percentiles of minimum and maximum temperature.

We compute time series of global and hemispheric averages over land masses only, and, in the case of *frost days* and *growing season*, over extra-tropical latitudes only, defined as poleward of $\pm 30^{\circ}$. Linear trends were fitted to the last 40 years of the 20th century time series, and, separately, to the entire length of the 21st century time series. Significance of the trends was determined through a traditional Student-*t* test, where the standard deviation of the residuals was estimated by (Restricted) Maximum Likelihood, after assuming an autocorrelated process of first order – as supported by exploratory data analysis – superimposed to the linear trend, thus accounting for temporal correlation in the residuals. The Student-t test was determined appropriate, after checking the consistency of the distributions of the residuals with the Gaussian assumption, a consistency that we find always satisfied (i.e. for all combinations of indices/models/scenarios and for global averages

as well as northern and southern hemispheres' averages). This finding is supported by the law of large numbers: we are considering trends for time series that result from aggregating many gridpoints into global and hemispheric averages, and we expect the result of this averages to approximate a Gaussian distribution even if the individual quantities (i.e. the individual index time series at each grid location) have distributional characteristics that differ significantly from normal.

Figures 1 and 2, left column, present multi-model ensemble average time series of the temperature indices, globally averaged, and smoothed with a 10-year running average. The time series are the same in both figures. The shadings in Figure 1 represent year-to-year variation before the smoothing, while the shadings in Figure 2 represent inter-model variability, as one standard deviation of the ensemble average. These summary figures encapsulate the main points highlighted in the following discussion.

When estimating trends over the last 40 years of the 20th century, for global and hemispheric average time series, the nine models easily agree over the sign for all indices but one. The sole exception are the trends estimated for *xtemp range* over the southern hemisphere, with respect to which some models project positive changes, while others project negative changes. These trends, however, are significant for a majority of models only for *frost days* (decreasing, see first panels of Figures 1 and 2, left column) and *growing season* (increasing, as shown by the third panels of Figures 1 and 2, left column). Four out of nine models show a significant trend also for *heat waves* at the global scale (increasing, as shown in the fourth panels of Figures 1 and 2, left column), *xtemp range* (decreasing, see second panels) and *warm nights* (increasing, see fifth panels). In comparing the significance of these trends with that calculated for observed trends in F02 it is important to note that estimation of the significance in that study does not seem to take into account the correlation in the residuals. This could explain the discrepancy with respect to our results: had we simply estimated trends by ordinary least squares, all the indices in all models would show a significant trend in the last four decades of the 20th century, at least at the global level of spatial aggregation. We also note that Kiktev et al. (2003) addressed this issue in their study of six of the ten indices, finding largely consistent results with the F02 study, although neither *heat waves* nor *xtemp range* were included in the subset of indices considered. The results of the comparisons between observed and model-simulated trends over the last 40 years of the 20th century are summarized in Table II.

When it comes to future projections, the trends in temperature-related indices first seen over the historical period – even in the cases where they were deemed not significant – become stronger and significant in all cases, as clearly shown in all panels of the left-hand columns in Figures 1 and 2. As in the 20th century, increases are projected for warm extremes and decreases for cold extremes, consistent with the general warming in these models associated with increasing greenhouse gas emissions. Common to all simulations is the fact that the trajectories for B1, the lower emissions scenario, separate from (i.e., display a relatively flatter trend than)

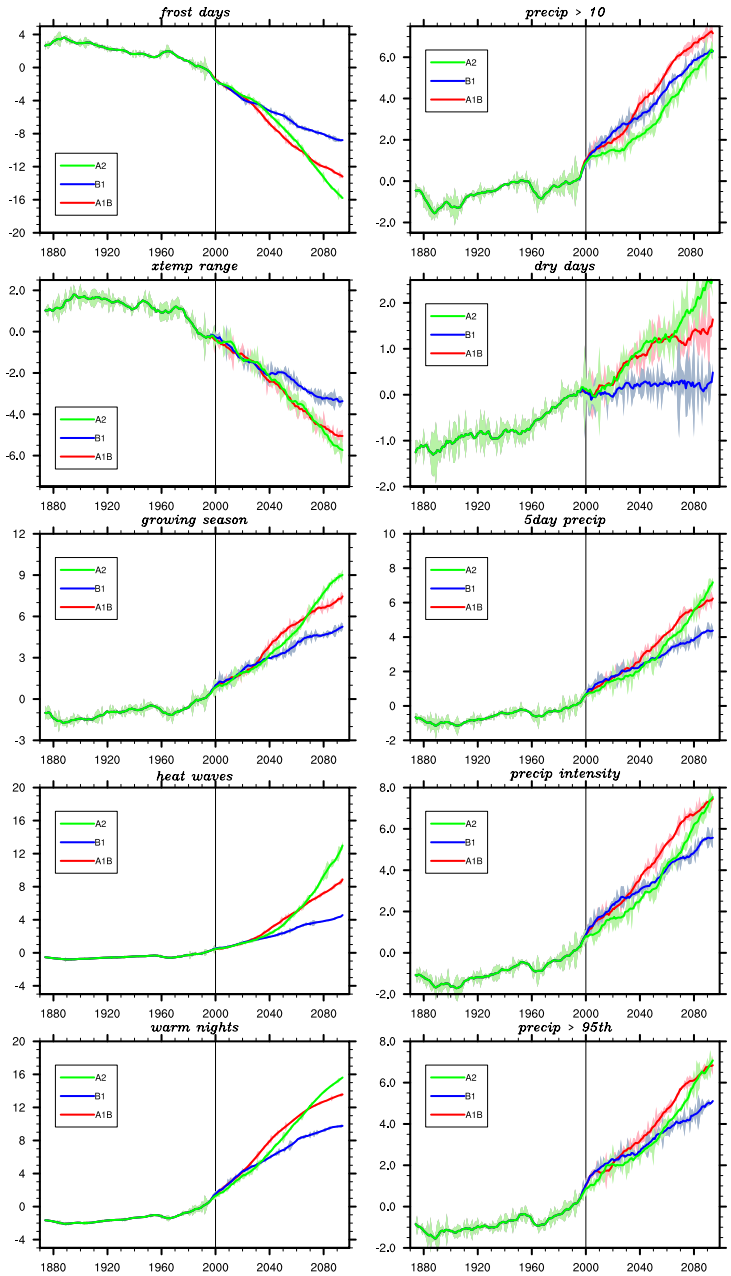

Figure 1. Time series of globally averaged (land only) values of temperature (left column) and precipitation (right column) extremes indices. Three SRES scenarios are shown in different colors for the length of the 21st century. The values have been standardized for each model as described in the main text, then averaged and smoothed by a 10-yr running mean. The envelope of year-to-year variation before the 10-yr smoothing is shown as background shading.

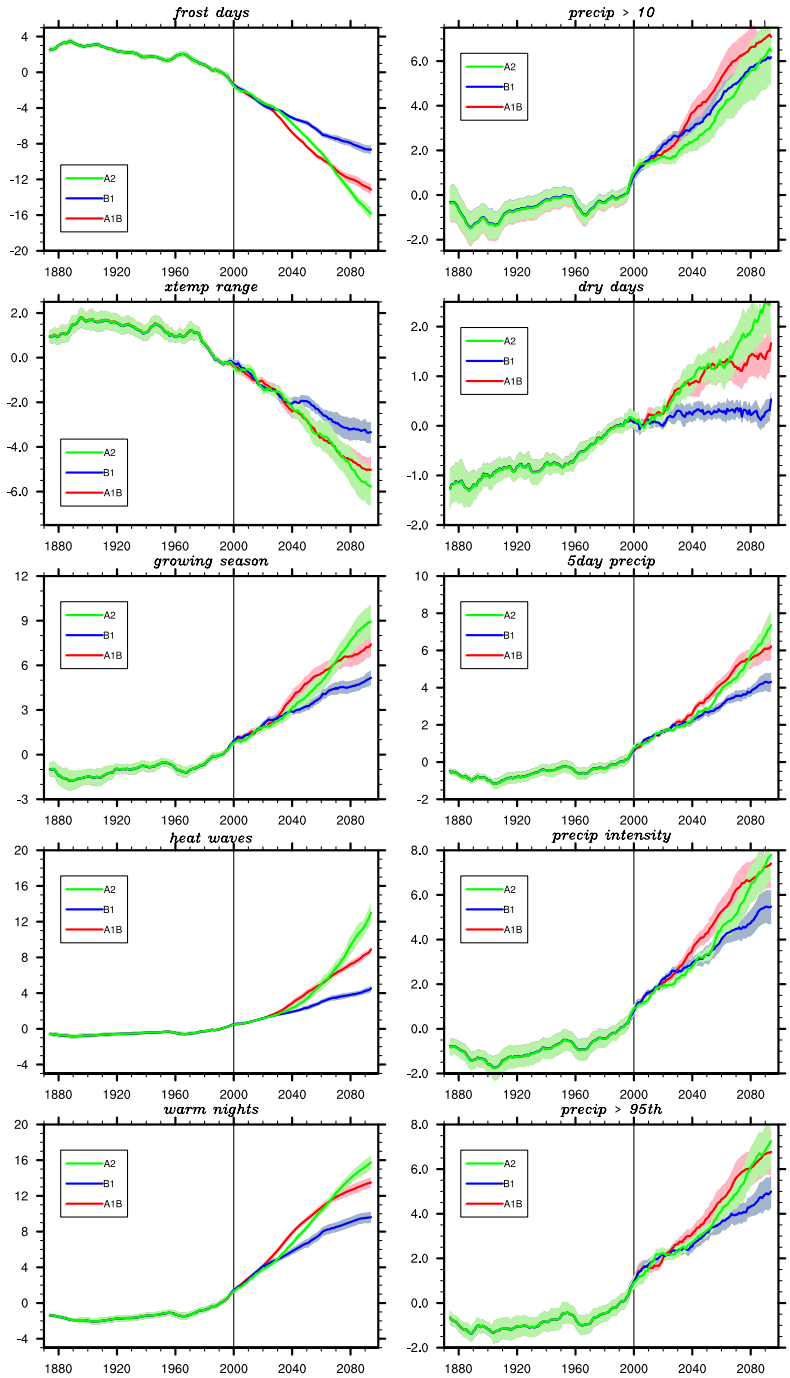

Figure 2. Same as Figure 1, but the shading here represents one standard deviation of the ensemble mean, as a measure of inter-model variability.

TABLE II
Summary of comparisons between observed and simulated trends (1960–2000) at the global average scale, discussed in Sections 3 and 4

Index	Observed trends	Simulated trends
Frost days	Significant decreasing trend	Decreasing trend in all models Significant for a majority (Same for hemispheric averages)
Xtemp range	Significant decreasing trend	Decreasing trend in all models Significant for four models (SH sees disagreement in sign among models)
Growing season	Significant increasing trend	Increasing trend in all models Significant for a majority (Trends in SH flat for most models)
Heat waves	No significant trend	Increasing trend in all models Significant for four models (Same for hemispheric averages)
Warm nights	Significant increasing trend	Increasing trend in all models Significant for a majority (Same for hemispheric averages)
Precip >10	Significant increasing trend	Increasing trend for all models Significant for a minority High inter-annual and inter-model variability
Dry days	Significant decreasing trend	Increasing trend for all models Significant for a minority High inter-annual and inter-model variability
5 day precip	Significant increasing trend	Increasing trend for all models Significant for a minority High inter-annual and inter-model variability
Precip intensity	No significant trend	Increasing trend for all models Significant for a minority High inter-annual and inter-model variability
Precip >95th	No significant trend	Increasing trend for all models Significant for a minority High inter-annual and inter-model variability

the steeper trajectories of A2 and A1B only well into the 21st century, around 2040. This is consistent with estimates of the time of separation in global mean temperature projections under different scenarios due to the lag in climate response and buildup of CO_2 from historical emission patterns (Stott and Kettleborough, 2002; Meehl et al., 2005b). The higher emission scenarios A1B and A2 seem to track each other for the greater part of the 21st century in most of the model simulations, at a higher rate of increase (for *heat waves*, *warm nights* and *growing season*) or decrease (*xtemp range* and *frost days*) than B1. These higher forcing runs separate only in the latter part of the 21st century, if at all. Results based on these three scenarios (which can be classified as lower, mid, and mid-high relative

to the full SRES range) clearly highlight the influence of emissions scenarios on the rate of change, suggesting that if this analysis were to be reproduced for an even lower scenario (e.g., stabilization of GHGs at current-day levels), the projected trends would likely diverge even further from the A2 and A1B scenarios than the B1 projections, and show slower rates of increase.

When time series of hemispheric averages are computed for the 21st century simulations, *warm nights* is the only index where the trends in the NH and in the SH have comparable rates of increase. For *frost days* and *growing season* the trends are significant in both hemispheres, but significantly steeper in the NH than in the SH as would be expected given the greater land mass and higher preponderance of continental interiors removed from the moderating effects of the ocean. The same is true with increasing trends for *heat waves*. When *xtemp range* is considered, the SH actually shows either little change (not significant) or even slightly increasing and significant trends (again perhaps reflecting the higher proportion of ocean area in that hemisphere), but the strongly decreasing and significant trends in the NH prevail in the global average. For the indices characterized by steeper trends in the NH than in the SH, the separation between scenarios also appears to be sharper in the NH than in the SH, especially between the lower-emission B1 and the higher-emission pair, A2 and A1B. This behavior confirms a more general conclusion: for quantities showing the steeper trends as a result of anthropogenic forcing, the emission scenarios separate relatively faster and to a greater degree than for quantities whose rate of change is smaller.

As already noted, Figures 1 and 2, left column, are graphical summaries of the above discussion, showing multi-model averages of smoothed time series for each index and scenario. Each model's simulated time series of globally averaged values for each index and scenario has been centered with respect to the 1980–1999 period's average. Then the standard deviation over the entire 1960–2100 period (after detrending) is used to standardize the series before aggregation, in order to adjust for different absolute magnitudes of the simulated indices among the different models (consistent with the general focus of this study on only the direction and significance of the changes, and the inter-model agreement on those). A 10-year running mean is applied to smooth the final time series, and the year-to-year variation (in Figure 1) and the ensemble mean's standard deviation (in Figure 2) are shown as a shading. Hemispheric average time series and single model, non-standardized time series are available from `http://www.cgd.ucar.edu/ccr/publications/tebaldi-extremes.html`.

3.2. GEOGRAPHICAL PATTERNS OF CHANGE

Our analysis at the geographical level focuses on the patterns of change resulting from the difference between the average values over the last 20 years of the 21st century (2080–2099) and the last 20 years of the 20th century (1980–1999). Consistent

with the fact that these indices are mild definitions of extremes and direct derivations of temperature fields, we found that the geographical patterns of changes for the individual indices across the three SRES scenarios for each model appear to be just modulations of a generally stable geographical pattern of temperature change. The pattern of change appears to scale with atmospheric CO_2 concentrations, such that the pattern obtained under the A2 scenario is a stronger version of that under A1B, and similarly A1B is a stronger version of what is seen under B1 for that same model. This lends support to projections made using a pattern scaling approach (Mitchell, 2003; Watterson and Dix, 2005) and is in agreement with previous findings that temperature-related impacts and indices tend to scale with the magnitude of GHG emissions (Hayhoe et al., 2004). In addition, the primary/dominant patterns of change are relatively uniform and robust across the models examined, thus also lending support to the hypothesis that these results will be representative, to some degree, of the remainder of the AR4 multi-model AOGCM ensemble.

Due to the relatively consistent patterns of geographical change and their apparent scaling with CO_2 emissions, we next describe the salient features common to all models and without reference to a specific SRES scenario. This is of course a generalization, but we limit our discussion to the most robust and strongest features that appear to be consistent across all the AOGCMs examined. The significance of the regional changes was tested by a Student-*t* test. We computed standard deviations on the basis of the interannual variability of each of the model/index combination over the part of the historical run showing no significant trend (i.e. 1900–1949), rescaled by the effective number of observations. For the latter, we performed an analyisis of the autocorrelation of the gridpoint time series, thus determining the lag in years by which subsequent fields generated by the model for a specific index simulation can be considered uncorrelated (a lag of one was sufficient in the great majority of cases). Aware of the issue of multiple testing when addressing the significance of geographical fields, we set the bar high by deeming significant only areas where the *t*-statistics were larger than 3 in absolute value (corresponding to an α-level of 0.0025). This, together with the inter-model consistency of the patterns, gives us confidence that the regional changes here highlighted have a high degree of robustness, at least within the current multi-model ensemble.

Figure 3, left column, synthesizes our discussion in 5 plots of the geographical changes under the A1B scenario, obtained as a multimodel average where the procedure applied to the time series of Figure 1 is applied gridpoint by gridpoint. These should then be considered only qualitative depiction of regional changes as they appear from the aggregation of the single-models results after the model-specific magnitude of the changes has been standardized. The dotted regions highlights areas where at least five models in the ensemble show a significant change according to the Student-*t* test at the α-level of 0.0025. A series of model- and scenario-specific geographical plots

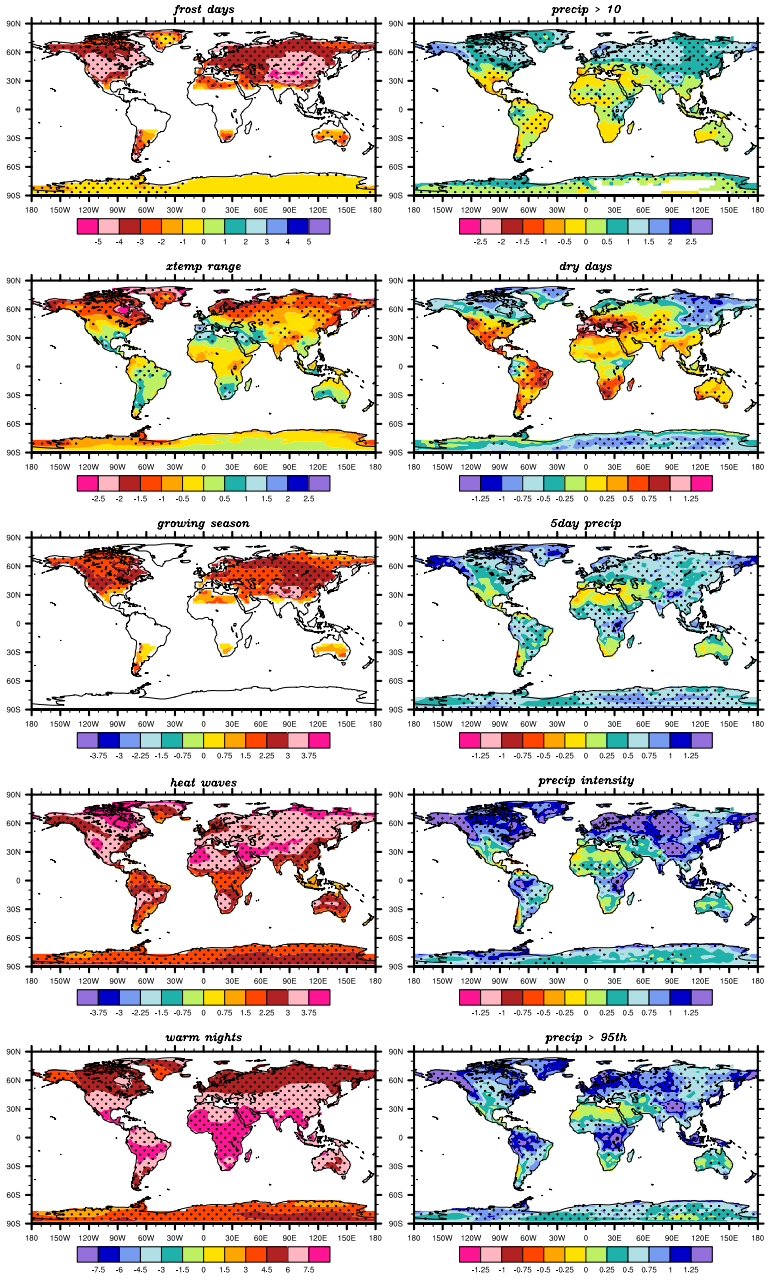

Figure 3. Multi-model averages of spatial patterns of change under A1B. Shown is the difference between two twenty-year averages (2080–2099 minus 1980–1999). Each gridpoint value for each model has been standardized first, then a multi-model simple average is computed. Stippled regions correspond to areas where at least five of the nine model concur in determining that the change is statistically significant. Oceans (and subtropical regions for *frost days* and *growing season*) are left blank because we chose not to include them in the analysis.

are available from http://www.cgd.ucar.edu/ccr/publications/tebaldi-extremes.html.

Frost days patterns (first panel, left column of Figure 3) follow the results described in Meehl et al. (2004), with a stronger decrease over the high latitudes of North America, propagating southward along the western edge of the continent. Thus, a negative gradient North to South and West to East characterize this index change over North America. For Europe and Asia the decrease is weaker along the Atlantic and Mediterranean coasts. The largest decreases are in the Scandinavian regions, and in most models following the topography of the higher elevations of Central Asia and Tibet. The North-Eastern part of Asia shows a less substantial decrease. The southern tips of South America and Africa see the largest decreases compared to other areas of those continents, consistent with the patterns of change in global mean temperatures which are greater at higher latitudes. The same applies to the southern latitudes of Australia. All the extratropical regions for which this index has a meaningful application see significant decreases by the end of the 21st century. As noted by Meehl et al. (2004), the pattern of these changes relates to the fact that decreases of frost days will be greater near the climatological mean position of the 0C isotherm, such that small changes near this boundary will result in relatively greater decreases in frost days in those regions. At higher latitudes, temperatures will continue to go below freezing irregardless of the warming such that nighttime temperatures still consistently go below freezing. Greater decreases of frost days along the western margins of the continents are related to changes in atmospheric circulation, with more warm moist westerly inflow from the oceans in the warmer climate producing relatively greater decreases of frost days in these regions (Meehl et al., 2004).

Xtemp range patterns (second panel, left column of Figure 3) show changes of both signs, despite the fact that the globally averaged index shows a significant downward trend consistent with greater increases in nighttime minima compared to daytime maxima found in other models but with spatial differences among models (e.g. Cubasch et al., 2001). Negative changes are consistently simulated over the higher latitude regions of the northern hemisphere. However, models show a consistent positive change over the South East U.S. and the Mediterranean basin, up to the mid-latitude regions of Europe. The regions of the southern hemisphere show mixed patterns, with large regions of positive changes, especially in most of South America, South Africa and Australia. Even if consistently simulated across models, the individual significance of these changes is less uniform than for the other indices. The majority of models deems significant the negative changes over the high latitudes of the northern hemisphere and a number of smaller regions in the lower latitudes and the southern hemisphere, characterized by positive changes. A more complete understanding of these changes would require a detailed analysis of changes in diurnal temperature range and the multiple processes affecting patterns of those changes. This is beyond the scope of this paper, but will be addressed in a subsequent study.

For *growing season* (third panel, left column of Figure 3) the significant patterns are opposite in sign to the changes in frost days, if somewhat less pronounced, modulating a general increase of the index over all the land masses. Over the U.S. a "belt" of relatively larger values, consistent across all models, appears over the Northwest, following the Pacific coast and then along the southern regions to the Atlantic coast. This pattern is clearly related qualitatively to the pattern of changes in frost days noted above, even if changes in night-time minima are not the only factor affecting changes in *growing season* length. For similar reasons, relatively larger values of the change are also simulated over Eastern Europe, the higher elevation regions of Central Asia, the southern tip of South America, and southeast Australia. With regard to the latter, it was pointed out however in F02 that the temperature-based index is not as relevant for areas such as the Australian continent, where the mild climate puts a larger relevance on precipitation amounts rather than temperature in determining the length and timing of the growing season. The changes simulated are all significant for the mid- and high latitudes of the northern hemisphere, but less consistently so across models in the southern hemisphere.

For *heat waves* (fourth panel, left column of Figure 3), a general significant increase over the land masses is also observed with large positive values over the southwest U.S., a finding that is supported by other recent studies (Hayhoe et al., 2004a,b; Meehl and Tebaldi, 2004). These changes are related to large mean temperature increases over land areas, with elements of the pattern associated with changes in atmospheric circulation with increased GHGs (Meehl and Tebaldi, 2004). Other patterns consistent across models are a relatively larger increase over North and central Australia and the high latitudes of the Asian continent, also related to changes in mean temperature outlined in other studies (e.g. Meehl et al., 2005b). The patterns over the West European and Mediterranean regions and Africa are not as consistent within the ensemble, with some models placing an area of large intensification over northern Europe and others expanding it all the way down to the Mediterranean basin and Balcans (consistent with similar findings by Meehl and Tebaldi, 2004).

The values of the change in *warm nights* (fifth panel, left column of Figure 3) are consistently positive and significant all over the globe, with generally an equator-to-poles negative gradient that is particularly pronounced in the southern hemisphere.

4. Precipitation Extremes

4.1. GLOBAL AND HEMISPHERIC AVERAGES

The analysis of observed historical changes in precipitation extremes indicators by F02 produced a picture of a world with intensifying precipitation events, even in the presence of less coherent spatial patterns – when compared to the

temperature-related indicators – as a consequence of the small-scale, local character of precipitation.

The indices showing the largest, most significant and spatially coherent changes were found in F02 to be *precip* >10 and *5 day precip*, both indicators of intensifying precipitation. That is, for a given precipitation event, proportionately more precipitation was recorded to fall in a warmer climate. This change is consistent with warmer oceans evaporating greater amounts of moisture, and the warmer air being able to hold more moisture. When this moister air moves over land, more intense precipitation is produced (Meehl et al., 2005a). A significant trend downward was found in *dry days*, describing a tendency towards less extended dry periods (i.e. more frequent rain events). The trends over the latter part of the 20th century for *precip intensity* and *precip* >95th, were not significant, but their sign too pointed in the direction of a wetter (and more extremely so) global climate.

A number of other studies have found changes in precipitation-related indices around the globe that vary by location. For example, Kiktev et al. (2003) found no change in *5 day precip* but some increases in *precip* >95th and decreases in *dry days*. Other studies found increases in heavy rainfall events as measured by decreasing return periods or increasing rainfall intensity in the western U.S. (Kim, 2005), the Caribbean (Peterson et al., 2002), the U.K. (Fowler and Kisbey, 2003), and Italy (Brunetti et al., 2004). However, in contrast to projected changes in temperature extremes, observed precipitation changes were found to exhibit strong local to regional-scale variability (e.g., U.K. – Ekstrom et al., 2005; New Zealand -Salinger and Griffiths, 2001; South East Asia – Manton et al., 2001).

The ensemble average time series summarizing our findings can be seen in Figures 1 and 2, right columns. The model simulations for the last 40 years of the 20th century are consistent with the findings in F02 with regard to the sign of the trends where the intensification of precipitation is concerned. The four indices measuring the intensity of rainfall events, *precip* >10 (first panels, right column of Figures 1 and 2) *5 day precip* (third panels), *precip intensity* (fourth panels) and *precip* >95th (fifth panels), all show positive trends in the aggregated time series, even if individual index/model combinations may not deem the trend significant, due to the large year-to-year variability of the global and hemispheric means. Thus, the intermodel spread around the ensemble average of these indices appears large, as can be assessed from the shading in Figure 2. For *dry days* (second panels, right column of Figures 1 and 2) the model average shows an increasing trend, contrary to the observed records, but the inter-model variability and the interannual variability are large for this index as well.

When it comes to future projections over the entire 21st century, the models do agree on both the positive sign and the significance of the trends for all of the indices measuring rainfall intensity, as clearly shown in the corresponding panels of Figures 1 and 2 – although whether this is a reflection of greater scientific certainty or merely similar assumptions underlying the physical parameterizations of the models examined remains to be seen. Nonetheless, this is physically consistent

with the warmer air in the future climate being able to hold more moisture. The increasing trends of the wet indices all show a larger positive slope in the course of the 21st century simulations, compared to the trend observed in the last part of the 20th century in association with the greater increases of temperature and thus increased moisture-holding capacity of the air. For *dry days* (second panels of the right columns in Figures 1 and 2) the majority of models continue to project a flat global and hemispheric average trend for the lowest emission scenario, B1 (with the exception of the GFDL models, predicting a significant increase), while significant increases are predicted under A2 and A1B.

Compared to the temperature indices, the separation of the trajectories of a given precipitation index under the different scenarios appears less cleanly, as a consequence of higher inter-model and interannual variability. It should also be noted that the steepness of the 21st century trends in the precipitation indices does not always scale with the strength of the emissions, i.e. the A1B precipitation index exhibits a stronger trend than the A2 index. This could in part be attributable to the smaller number of A2 than A1B experiments in the model ensemble. In particular, MIROC3.2 (hires) exhibits the strongest trends in most of the precipitation indices under A1B, and CCSM3 exhibits the strongest trend for *precip* >10 under A1B, and neither model provided indices from the A2 experiment.

Table II presents a summary of the comparisons of observational-based trend estimates with historical model simulations.

When considering northern and southern hemispheres separately, generally the precipitation-indices trends appear of consistent sign, and most often of not significantly different slopes. Hemispheric average time series and single model, non-standardized time series are available from `http://www.cgd.ucar.edu/ccr/publications/tebaldi-extremes.html`.

4.2. GEOGRAPHICAL PATTERNS OF CHANGE

Figure 3, right column, shows graphical summaries for the five precipitation indices of the geographical patterns of change and the multi-model consensus over their significance. The full spectrum of model- and scenario-specific geographical plots are available from `http://www.cgd.ucar.edu/ ccr/publications/tebaldi-extremes.html`.

There is no a priori reason to assume that different emission scenarios will result in scalable precipitation extremes. On the other hand, results from a study of average precipitation under different scenarios that applied pattern scaling (Tebaldi et al., 2002) found very good agreement among geographical patterns of average precipitation change under SRES A2, A1B and B2.

In fact, we also find that for the five precipitation indices, as for the temperature indices, the geographical patterns of change between the last 20 years of the 20th

century and the last 20 years of the 21st century do appear similar across scenarios although they do not always increase in magnitude with emissions, suggesting perhaps that they are more a function of model dynamics and parameterization and how the model responds to forcing than to emission scenarios per se. Intensification of the rainfall amounts, as measured by *5 day precip*, *precip intensity* and *precip* >95th (third, fourth and fifth panels, right column of Figure 3) produces positive changes over all the land masses. These changes are deemed significant by a majority of models across the mid- to high latitudes of the northern hemisphere and the tropical regions of South America and Africa. Reasons for this pattern are likely related to two factors: (1) proportionately more precipitation and precipitation intensity in areas of existing storm tracks and associated dynamical moisture convergence resulting simply from the greater moisture holding capacity of the warmer air, and (2) a slight poleward shift of the midlatitude storm tracks (e.g. Meehl et al., 2005a; Yin, 2005).

Coherent patterns emerge from the multi-model average for *precip* >10 and *dry days* (first and second panel of Figure 3), but the significance of these changes is much less uniform than for the other indices. The nine models show large areas of both negative and positive change. The mid- and high latitudes of the northern hemisphere see an increase in *precip* >10 and at the same time a shortening, on average, of the length of the dry spells. The lower latitudes of the northern hemisphere and the southern hemisphere see a tendency towards longer dry spells, associated to changes in *precip* >10 of both signs, the latter not consistent across models. The regions of significant change in either indices by a majority of models are very few and have a finer scale than the ones highlighted for the other precipitation indices. Low latitudes and southern hemisphere in general are areas where mean rainfall is projected as decreasing across the models (Meehl et al., 2005a). Thus, even though precipitation intensity increases in those regions, there are longer periods between rainfall events (more consecutive dry days) and a decrease in average rainfall. In other words, it rains less frequently, but when it does rain, there is more precipitation for a given event.

5. Twentieth Century Geography of Change in Simulations

Figure 4 shows geographical patterns of changes computed as standardized differences between 1980–1999 and 1900–1919 to provide a comparison of these spatial changes with the changes computed for the future.

For all the indices it is clear that the dominant patterns surfacing with significant strength at the end of the 21st century are the ones already present at the end of the 20th century. This is – not surprisingly – most evident in the temperature-related indices (left columns of Figures 3 and 4), but is detectable in the precipitation indices as well.

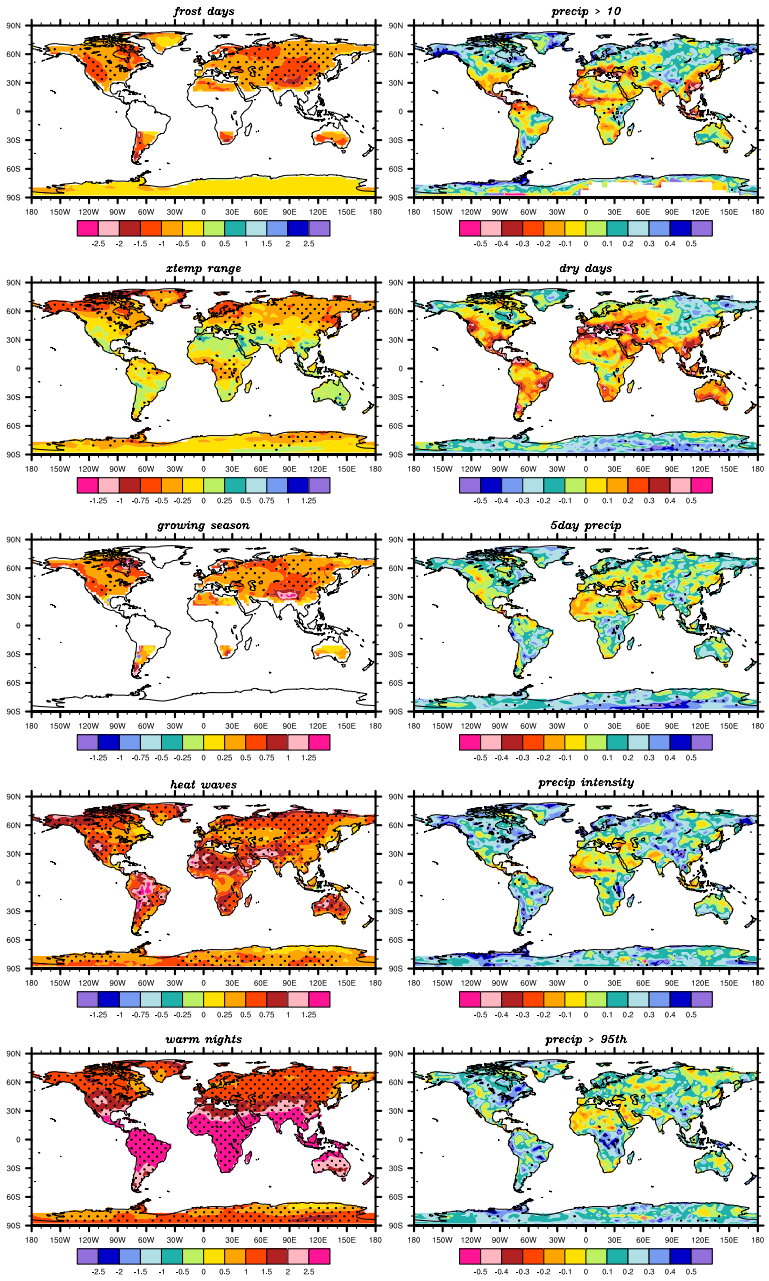

Figure 4. Multi-model averages of spatial patterns of change at the end of the 20th century. Shown is the difference between two twenty-year averages (1980–1999 minus 1900–1919). Each gridpoint value for each model has been standardized first, then a multi-model simple average is computed. Stippled regions correspond to areas where at least five of the nine model concur in determining that the change is statistically significant. Oceans (and subtropical regions for *frost days* and *growing season*) are left blank because we chose not to include them in the analysis.

With regard to the spatial coherence and the significance of these changes, our findings are consistent with what we have already discussed in this paper, and what F02 and Alexander et al. (2005) show on the basis of the observational data sets. Temperature indices show larger coherent areas of change, and of larger statistical significance than the precipitation indices. The stippling in Figure 4 shows areas where a majority of models have simulated statistically significant changes. Here we apply the same Student-*t* test that we applied to test significance for the changes at the end of the 21st century, depicted in Figure 3, but we lower the threshold to two standard deviations rather than three, thus to a nominal α-level of 0.05. The indices associated with changes in minimum temperature, *frost days* and *warm nights* and the *heat wave* index (first, fifth and fourth panels, left column of Figure 4) show wide consensus in the significance of the changes over most of the land areas, while *growing season* and *Xtemp range* see more limited areas of significance. The *Xtemp range* index is unique among the temperature indices in showing changes of both signs (even if the models do not attribute statistical significance to the positive changes), this fact too consistent with the projected changes over the 21st century.

None of the precipitation indices (right column of Figure 4) shows significant regions of change, even at this lower level of statistical significance. Nonetheless the patterns of change do represent a "preview" of what is in store for the next century, hinting at the fact that although the trend is still confounded by year-to-year variability and the inter-model spread, it is arguably already in existence.

6. Conclusions

When considering the simulation of extreme climate we do not yet expect models to accurately reproduce observed absolute quantities or rates of change: on the one side the still relatively coarse resolution of AOGCMs prevents the simulation of phenomena that manifest their intensity mainly at synoptic scales; on the other side, if we wanted to aggregate locally recorded extreme events over the typical model gridbox, arbitrary choices of aggregation and interpolation would be necessary. Thus, in this study, we did not analyse the agreement (both among models and compared to observed data) of model-simulated absolute values. This awaits the release of the new gridded observational extremes product by Alexander et al. (2005). Rather, our goal consisted primarily of determining if results from different climate model simulations can support general statements in terms of tendencies for the future climate, and if they are physically consistent with what we would expect to occur given the processes known to be relatively well-simulated in the models. Thus, we chose to evaluate the sign of current (defined as the last 40 years of the last century) and future (over the entire 21st century) trends, and geographical patterns of change (defined as the difference between the last 20 years of 20th and 21st centuries), focusing on statistical significance of the sign of change, agreement with observed tendencies and inter-model agreement.

Our analysis enables a number of conclusions to be drawn, namely:

- Models agree well with observations that there has already been a trend in temperature-related extremes in the positive direction for *growing season, heat waves* and *warm nights* and in the negative direction for *frost days*, and *xtemp range* – the latter at least at the global scale of aggregation, dominated by the behavior of the index in the northern hemisphere – consistent with the notion of a warming climate.
- Over the next century, all models show a continued trend for more extremes in the temperature-related extremes indices. This trend is of the same sign but greater magnitude than observed over the past century, and again is consistent with a warming climate due mainly to increases of anthropogenic GHGs.
- Projected geographical changes in temperature extremes are relatively consistent across models and appear to scale with emissions scenario (demonstrating a strong relationship between GHG emissions and the magnitude of potential impacts as reflected by the temperature indices). In particular, "hot spots" include the following:

  - The high latitudes of the northern hemisphere for most of these indices, as a general consequence of the higher rate of warming already documented in many studies of climate change. In particular for *xtemp range* the largest significant negative changes are concentrated over these areas.
  - The northwest region of North America, particularly for decreases in *frost days* and increases in *growing season* length and the Southwest for increasing incidence of *heat waves*, related mainly to changes in atmospheric circulation with increasing GHGs.
  - Eastern Europe for the larger increases in *growing season* and decreases in *frost days* over that continent, again related mainly to changes in atmospheric circulation.
  - Northern Australia for the largest increases in *heat waves* over that continent, and Australia's South East for the largest changes in *frost days* (decreasing) and *growing season* (increasing).

- Models also agree with observations over the historical period that there is a trend towards a world characterized by intensified precipitation, with a greater frequency of heavy-precipitation and high-quantile events, although with substantial geographical variability.
- The high latitudes of the northern hemisphere show the most coherent regional patterns of significant positive changes in the intensity of wet events, defined through four of the precipitation extremes indices: *precip* >10, *5 day precip*, *precip* >95th and *precip intensity*. These changes are related to the greater moisture-holding capacity of the warmer air contributing to greater moisture convergence, as well as a poleward shift of the storm tracks.

– The index intended to measure dry spell duration, *dry days*, shows a positive global trend in future projections only for the higher emission scenarios, B1 producing a flat time series for the index in the future. This is the index showing the largest relative interannual and inter-model variability. Regional patterns seem to differentiate high latitudes of the northern hemisphere, where negative changes are consistently predicted even if the significance remains at best spotty, to the lower subtropical latitudes of the same hemisphere, and the southern hemisphere, where positive changes predominate. However, as noted previously, the *dry days* index is not adequate to capture the kind of sustained drought conditions that would have severe impacts on water availability for most human systems. For this reason, this index is perhaps more useful to complement the *precip* >10, *5 day precip*, *precip* >95th and *precip intensity* indices in identifying changes in the proportion of wet and dry days and the distribution of rainfall. Taken together, these five indices offer a picture of regions whereby little to no change in mean precipitation could mask a simultaneous increase in both dry day periods and heavy rainfall events conducive to flooding conditions (Kunkel, 2003; Kunkel et al., 1999).

Estimates of changes in temperature and precipitation extremes, as presented here, are of key importance to assessments of the potential impacts of climate change on human and natural systems. In the past, such assessments have often had to depend on projected changes in climate means (USGCRP, 2000) despite the fact that it is the climate extremes that currently cause the most weather-related damages (Kunkel et al., 1999; Easterling et al., 2000; Meehl et al., 2000). In the future, rising frequency, intensity and duration of temperature extremes – both individual days, as represented by *warm nights*, as well as extended periods of extreme heat, as represented by *heat waves* – are likely to have adverse effects on human mortality and morbidity (McMichael and Githeko, 2001). Changes in precipitation-related extremes such as heavy rainfall and associated flooding also have the potential to incur significant economic losses and fatalities (Kunkel et al., 1999). Natural systems will likely be affected by changes in both temperature and precipitation extremes, as these have been shown to cause shifts in ecosystem distributions, trigger extinctions, and alter species morphology and behaviour (Parmesan et al., 2000).

Estimating future potential changes in both temperature and precipitation extremes provides essential input to urban, regional and national adaptation and planning strategies through the establishment of, for example, heat watch-warning systems or flood prevention strategies (e.g., Sheridan and Kalkstein, 2004; Hawkes et al., 2003). Our hope is that the analysis presented here, which attempts to highlight both areas of agreement as well as uncertainty, contributes to this effort.

Acknowledgements

We acknowledge the international modeling groups for providing their data for analysis, the Program for Climate Model Diagnosis and Intercomparison (PCMDI) for collecting and archiving the model data, the JSC/CLIVAR Working Group on Coupled Modelling (WGCM) and their Coupled Model Intercomparison Project (CMIP) and Climate Simulation Panel for organizing the model data analysis activity, and the IPCC WG1 TSU for technical support. The IPCC Data Archive at Lawrence Livermore National Laboratory is supported by the Office of Science, U.S. Department of Energy. Portions of this study were supported by the Office of Biological and Environmental Research, U.S. Department of Energy, as part of its Climate Change Prediction Program, and the National Center for Atmospheric Research. This work was also supported in part by the Weather and Climate Impact Assessment Initiative at the National Center for Atmospheric Research. The National Center for Atmospheric Research is sponsored by the National Science Foundation. Katharine Hayhoe was partially supported by the United States Environmental Protection Agency through *Science to Achieve Results* (STAR) Cooperative Agreement no. R-82940201, at the University of Chicago, Center for Integrating Statistical and Environmental Science. The authors thank Dr. Gabi Hegerl and two anonymous reviewers for their positive and constructive feedback.

Notes

1. See Johns et al., 2004 for a model description and analysis of preliminary experiments with HadGEM1 for the IPCC Forth Assessment Report, available online at `http://www.metoffice.com/research/hadleycentre/pubs/HCTN/HCTN55.pdf`
2. Although a low correlation between the chosen indices is also desirable in order to elevate the individual relevance of each index, to our knowledge no assessment has yet been performed of the correlation (or lack thereof) between the ten F02 indices. In terms of temperature, some correlation is inevitable regardless of the type of index chosen in that all indices reflect a warming climate. F02 find similar patterns of spatial change for all temperature indices, while both historical observed (F02) and future modelled indices (this study) indicate consistent changes in temperature indices indicative of an overall warmer climate. For precipitation, much more mixed results are seen, suggesting an overall lower correlation between the individual indices as well as between the models and observations.
3. The PCMDI archive is accessed through `http://www-pcmdi.llnl.gov`
4. Publications related to CCSM3 are available at `http://www.ccsm.ucar.edu/publications/`
5. Documentation is online at `http://www.ccsr.u-tokyo.ac.jp/kyosei/hasumi/MIROC/tech-repo.pdf`
6. Documentation is available through `http://www-pcmdi.llnl.gov`

References

Adamowski, K. and Bougadis, J.: 2003, 'Detection of trends in annual extreme rainfall', *Hydro. Proc.* **17**, 3547–3560.

Alexander, L.V., Zhang, X., Peterson, T.C., Caesar, J., Gleason, B. et al.: 2005, 'Global observed changes in daily climate extremes of temperature and precipitation', *Submitted*.

Bohm, U., Kucken, M., Hauffe, D., Gerstengarbe, F., Werner, P. et al.: 2004, 'Reliability of regional climate model simulations of extremes and of long-term climate', *Nat. Haz. & Earth Sys. Sci.* **4**, 417–431.

Brunetti, M., Buffoni, L., Mangianti, F., Maugeri M., and Nanni, T.: 2004, 'Temperature, precipitation and extreme events during the last century in Italy', *Global & Planet. Change* **40**, 141–149.

Delworth, T. L., Stouffer R., Dixon R. et al.: 2002, 'Review of simulations of climate variability and change with the GFDL R30 coupled climate model', *Clim. Dyn.* **19**, 555–574.

Diansky, N. A. and Volodin, E. M.: 2002, 'Simulation of present-day climate with a coupled atmosphere-ocean general circulation model', *Izvestiya* **38**, 732–747.

Dixon, K. W., Delworth, T., Knutson, T., Spelman M., and Stouffer, R.: 2003, 'A comparison of climate change simulations produced by two GFDL coupled climate models', *Global & Planet. Change* **37**, 81–102.

Duffy, P. B., Govindasamy, B., Iorio, J. P., Milovich, J., Sperber, K. R., Taylor, K. E.,Wehner M. F., and Thompson, S. L.: 2003, 'High-resolution simulations of global climate, part 1: Present climate', *Clim. Dyn.* **21**, 371–390.

Easterling, D. R., Meehl, G. A., Parmesan, C., Changnon, S. A., Karl, T. R., and Mearns, L. O.: 2000, 'Climate extremes: Observations, modeling, and impacts', *Science* **289**, 2068–2074.

Ekstrom, M., Fowler, H., Kilsby, C., and Jones, P. D.: 2005, 'New estimates of future changes in extreme rainfall across the UK using regional climate model integrations. 2. Future estimates and use in impact studies', *J. Hydrology* **300**, 234–251.

Fowler, H. J. and Kilsby, C. G.: 2003, 'A regional frequency analysis of United Kingdom extreme rainfall from 1961 to 2000', *Intl. J. Clim.* **23**, 1313–1334.

Frich, P., Alexander, L. V., Della-Marta, P., Gleason, B., Haylock, M., Tank, A. M. G. K. and Peterson, T.: 2002, 'Observed coherent changes in climatic extremes during the second half of the twentieth century', *Clim. Res.* **19**, 193–212.

Gao, X. J., Zhao, Z. C. and Giorgi, F.: 2002, 'Changes of extreme events in regional climate simulations over East Asia', *Adv. Atmos. Sci.* **19**, 927–942.

Gong, D. Y., Pan, Y. Z. and Wang, J. A.: 2004, 'Changes in extreme daily mean temperatures in summer in eastern China during 1955–2000', *Theor. & Appl. Clim.* **77**, 25–37.

Govindasamy, B., Duffy, P. B. and Coquard, J.: 2003, 'High-resolution simulations of global climate, part 2: Effects of increased greenhouse cases', *Clim. Dyn.* **21**, 391–404.

Hare, B. (ed.): 2006, 'Key vulnerable regions and climate change', in *Proceedings of the International Symposium on 'Key Vulnerable Regions and Climate Change: Identifying Thresholds for Impacts and Adaptation in Relation to Article 2 of the UNFCC'*, in press.

Hawkes P., Surendran S., and Richardson, D.: 2003, 'Use of UKCIP02 climate-change scenarios in flood and coastal defence', *J. Chart. Inst. Water & Env. Mgmt.* **17**, 214–219.

Hayhoe, K., Cayan, D., Field, C., Frumhoff, P., Maurer, E. et al.: 2004, 'Emissions pathways, climate change, and impacts on California', *PNAS* **101**, 12422–12427.

Hegerl, G. C., Zwiers, F., Kharin, S., and Stott, P.: 2004, 'Detectability of anthropogenic changes in temperature and precipitation extremes', *J. Clim.* **17**, 3683–3700.

Houghton, J. T., Ding, Y., Griggs, D. J., Noguer, M., van der Linden, P. J., Dai, X., Maskell, K., and Johnson, C. A. (eds.): 2001, *Climate Change: The Scientific Basis. Contributions of Working Group 1 to the Third Assessment Report of the Intergovernmental Panel on Climate Change*. Cambridge University Press, Cambridge and New York, 881 pp.

Huth, R. and Pokorna, L.: 2005, 'Simultaneous analysis of climatic trends in multiple variables: An example of application of multivariate statistical methods', *Intl. J. Clim.* **25**, 469–484.

Katz, R. W. and Brown, B. G.: 1994, 'Sensitivity of extreme events to climate change – The case of autocorrelated time-series', *Environmetrics* **5**, 451–462.

Katz, R., Brush, G., and Parlange, M.: 2005, 'Statistics of extremes: Modeling ecological disturbances', *Ecology* **86**, 1124–1134.

Khaliq, M. N., St-Hilaire, A., Ouarda T., and Bobee, B.: 2005, 'Frequency analysis and temporal pattern of occurrences of southern Quebec heatwaves', *Intl. J. Clim.* **25**, 485–504.

Kharin, V. and Zwiers, F.: 2005, 'Estimating extremes in transient climate change simulations', *J. Clim.* **18**, 1156–1173.

Kiktev, D., Sexton, D., Alexander, L., and Folland, C.: 2003, 'Comparison of modeled and observed trends in indices of daily climate extremes', *J. Clim.* **16**, 3560–3571.

Kim, J.: 2005, 'A projection of the effects of the climate change induced by increased CO_2 on extreme hydrologic events in the western US', *Clim. Ch.* **68**, 153–168.

Kunkel, K. E.: 2003, 'North American trends in extreme precipitation', *Natural Hazards* **29**, 291–305.

Kunkel, K. E., Pielke R. Jr. and Changnon, S. A.: 1999, 'Temporal fluctuations in weather and climate extremes that cause economic and human health impacts: A review', *Bull. Am. Met. Soc.* **80**, 1077–1098.

Manton, M. J., Della-Marta, P., Haylock, M., Hennessy, K., Nicholls, N. et al.: 2001, 'Trends in extreme daily rainfall and temperature in Southeast Asia and the South Pacific: 1961–1998', *Intl. J. Clim.* **21**, 269–284.

McMichael, A. and Githeko, A.: 2001, 'Human Health' in *Climate Change 2001: Impacts, Adaptation and Vulnerability*, J. McCarthy et al. (eds.). Cambridge University Press, Cambridge, UK, pp. 451–485.

Meehl, G. A., Karl, T., Easterling, D., Changnon, S., Pielke R. Jr. et al.: 2000, 'An introduction to trends in extreme weather and climate events: Observations, socioeconomic impacts, terrestrial ecological impacts, and model projections', *Bull. Am. Met. Soc.* **81**, 413–416.

Meehl, G. A., Tebaldi C. and Nychka D.: 2004, 'Changes in frost days in simulations of twentyfirst century climate', *Clim. Dyn.* **23**, 495–511.

Meehl, G. A. and Tebaldi, C.: 2004, 'More intense, more frequent, and longer lasting heat waves in the 21st century', *Science* **305**, 994–997.

Meehl, G. A., Arblaster, J. M. and Tebaldi, C.: 2005a, 'Understanding future patterns of increased precipitation intensity in climate model simulations', *Geophys. Res. Lett.* **32**, Art. No. L18719.

Meehl, G. A., Washington, W. M., Collins, W. D., Arblaster, J. M., Hu, A., Buja, L. E., Strand, W. G. and Teng, H.: 2005b, 'How much more global warming and sea level rise?', *Science* **307**, 1769–1772.

Mitchell, T. D.: 2003, 'Pattern scaling – an examination of the accuracy of the technique for describing future climate', *Climatic Change* **60**, 217–242.

Nakicenovic, N. and Swart, R. (eds.): 2000, *Emissions Scenarios: A Special Report of Working Group III of the Intergovernmental Panel on Climate Change IPCC. Special Report on Emissions Scenarios*. Cambridge University Press, Cambridge and New York, 612 pp.

Nasrallah, H. A., Nieplova, E., and Ramadan, E.: 2004, 'Warm season extreme temperature events in Kuwait', *J. Arid Env.* **56**, 357–371.

Negri, D. H., Gollehon, N. R., and Aillery, M. P.: 2005, 'The effects of climatic variability on US irrigation adoption', *Climatic Change* **69**, 299–323.

Palmer, T. N. and Raisanen, J.: 2002, 'Quantifying the risk of extreme seasonal precipitation events in a changing climate', *Nature* **415**, 512–514.

Parmesan, C., Root, T. L., and Willig, M. R.: 2000, 'Impacts of extreme weather and climate on terrestrial biota', *Bull. Am. Met. Soc.* **81**, 443–450.

Peterson, T. C., Taylor, M., Demeritte, R., Duncombe, D., Burton, S. et al.: 2002, 'Recent changes in climate extremes in the Caribbean region', *J. Geophys. Res.* **107**, Art. No. 4601.

Prieto, L., Herrera, R., Diaz, J., Hernandez, E. and del Teso, T.: 2004, 'Minimum extreme temperatures over Peninsular Spain', *Global & Planet. Change* **44**, 59–71.

Raisanen, J. and Joelsson, R.: 2001, 'Changes in average and extreme precipitation in two regional climate model experiments', *Tellus A* **53**, 547–566.

Robeson, S.: 2004, 'Trends in time-varying percentiles of daily minimum and maximum temperature over North America', *Geophys. Res. Lett.* **31**, Art. No. L04203.

Rusticucci, M. and Barrucand, M.: 2004, 'Observed trends and changes in temperature extremes over Argentina', *J. Clim.* **17**, 4099–4107.

Ryoo, S. B., Kwon, W. T. and Jhun, J. G.: 2004, 'Characteristics of wintertime daily and extreme minimum temperature over South Korea', *Intl. J. Clim.* **24**, 145–160.

Salinger, M. J. and Griffiths, G. M.: 2001, 'Trends in New Zealand daily temperature and rainfall extremes', *Intl. J. Clim.* **21**, 1437–1452.

Semmler, T. and Jacob, D.: 2004, 'Modeling extreme precipitation events – a climate change simulation for Europe', *Global & Plan. Change* **44**, 119–127.

Sheridan, S. C. and Kalkstein, L. S.: 2004, 'Progress in heat watch-warning system technology', *Bull. Am. Met. Soc.* **85**, p. 1931.

Tank, A. M. G. K. and Konnen, G. P.: 2003, 'Trends in indices of daily temperature and precipitation extremes in Europe, 1946–99', *J. Clim.* **16**, 3665–3680.

Tebaldi, C., Nychka, D., and Mearns, L.O.: 2004, 'From global mean responses to regional signals of climate change: Simple pattern scaling, its limitations (or lack of) and the uncertainty in its results', *Proceedings of the 18th Conference on Probability and Statistics in the Atmospheric Sciences*, AMS Annual Meeting, Seattle, WA.

U.S. Global Change Research Program (USGCRP): 2000. *U.S. National Assessment of the Potential Consequences of Climate Variability and Change* Cambridge University Press, Cambridge, UK.

Washington, W. M., Weatherly, J. W., Meehl, G. A., Semtner, A. J., Bettge, T. W., Craig, A. P., Strand, W. G., Arblaster, J. M., Wayland, V. B., James, R., and Zhang, Y.: 2000, 'Parallel climate model (PCM) control and transient simulations', *Clim. Dyn.* **16**, 755–774.

Watterson, I. G. and Dix, M. R.: 2005, 'Effective sensitivity and heat capacity in the response of climate models to greenhouse gas and aerosol forcings', *QJRMS* **131**, 259–279.

Yin, J.: 2005, 'A consistent poleward shift of the storm tracks in simulations of 21st Century climate', *Geophys. Res. Lett.* **32**, Art. No. L18701.

Zhai, P. M. and Pan, X. H.: 2003, 'Trends in temperature extremes during 1951–1999 in China', *Geophys. Res. Lett.* **30**, Art. No. 1913.

(Received 3 June 2005; in revised form 21 December 2005)